Quantification of highly unsteady and inhomogeneous stratified turbulence in breaking internal waves on slopes

Robert S. Arthur[1,3], Presenting Author, S. Karan Venayagamoorthy[2,3], Jeffrey R. Koseff[3], and Oliver B. Fringer[3]

1. Department of Civil & Environmental Engineering, University of California, Berkeley (Presenting author email address: barthur@berkeley.edu)
2. Department of Civil & Environmental Engineering, Colorado State University
3. The Bob and Norma Street Environmental Fluid Mechanics Laboratory, Department of Civil & Environmental Engineering, Stanford University

Abstract

Direct numerical simulations are used to explore the mixing efficiency of breaking internal waves on slopes. Data from the study of Arthur et al. (2016), which include eight breaking wave cases with a range of initial pycnocline thicknesses but similar incoming wave properties, are considered. The mixing efficiency is quantified using an irreversible version of the flux Richardson number R_f^*, and variations in R_f^* are explored as a function of the buoyancy Reynolds number Re_b. Two different methods for computing the buoyancy frequency N, one based on a three-dimensionally resorted density field and the other based on locally-resorted vertical density profiles, are used to explore the effect of N on turbulence calculations. It is shown that how N is calculated changes not only R_f^*, but also the nondimensional quantity Re_b, leading to potential uncertainty in estimates of the mixing efficiency using Re_b-based parameterizations.

1 Introduction

Diapycnal mixing, or the molecular diffusion of density across isopycnal surfaces, is thought to be a primary control on the ocean stratification (Munk and Wunsch, 1998; Wunsch and Ferrari, 2004). Turbulent stirring enhances this mixing by deforming isopycnal surfaces, creating both sharper density gradients and a greater surface area over which molecular diffusion can occur. Turbulent stirring, therefore, is reversible, and represents an exchange between turbulent kinetic energy and available potential energy. Diapycnal mixing, however, is irreversible; it represents a sink of turbulent kinetic energy into the background potential energy of the ocean.

Because diapycnal mixing happens at small scales, it is difficult to capture in field measurements or to resolve in numerical models. A great deal of work has therefore gone into estimating mixing using more easily resolved quantities. Much of this work is based on the Osborn (1980) model for steady, homogeneous turbulence, $K_\rho = \left(\frac{R_f}{1-R_f}\right)\frac{\epsilon}{N^2}$, where K_ρ is the turbulent diffusivity of density, ϵ is the dissipation of turbulent kinetic energy, and N is the buoyancy frequency. The model also depends on the flux Richardson number $R_f = \mathcal{B}/(\mathcal{B}+\epsilon)$, where $\mathcal{B}$ is the turbulent buoyancy flux (Ivey and Imberger, 1991). R_f is often referred to as the mixing efficiency because it represents the fraction of turbulent kinetic energy production that goes into the turbulent buoyancy flux.

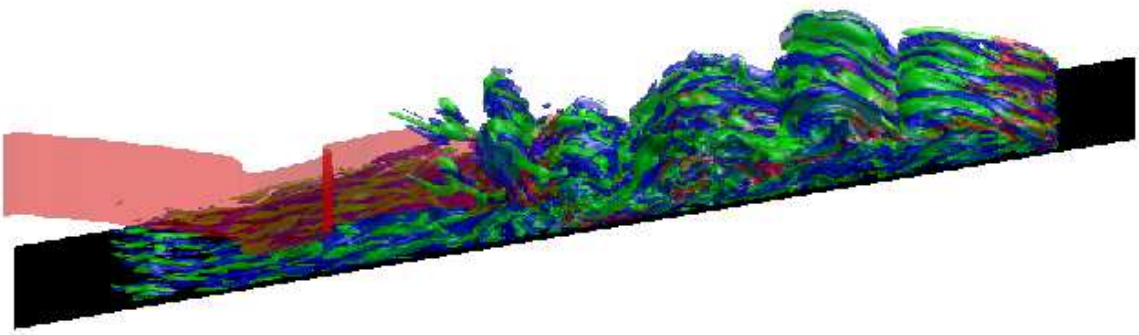

Figure 1: A three-dimensional view of the turbulent flow field during breaking for an internal wave with intermediate interface thickness (case 5 in Arthur et al., 2016). Isosurfaces of the reference density $\rho = \rho_0$ (red), positive streamwise vorticity $\Omega_1/\omega_1 = 37$ (blue), and negative streamwise vorticity $\Omega_1/\omega_1 = -37$ (green) are shown, where ω_1 is the frequency of the incoming wave.

While Osborn (1980) assumed a constant $R_f \approx 0.17$, many parameterizations for R_f have been developed based on nondimensional numbers that describe the state of the turbulence (e.g., Ivey and Imberger, 1991; Shih et al., 2005; Bouffard and Boegman, 2013). Due to the difficulties in calculating R_f in unsteady, inhomogeneous turbulence in the field, these parameterizations are generally based on the results of idealized laboratory experiments and direct numerical simulations (DNS). Several field studies (e.g., Davis and Monismith, 2011; Walter et al., 2014) have shown good agreement with existing parameterizations, while others (e.g., Lozovatsky and Fernando, 2013) have shown clear differences. The study of Mater and Venayagamoorthy (2014) provides a thorough summary of the current state of R_f parameterizations in the literature. However, the existence of a "universal" parameterization for R_f remains an open question.

In this work, the mixing efficiency of breaking internal waves on slopes is explored using the DNS dataset of Arthur et al. (2016). As highlighted in figure 1, breaking internal waves on slopes are an inherently unsteady, inhomogenous flow, and are thus a useful case study for calculating and interpreting R_f. Particular attention is paid to the method of calculating the buoyancy frequency N, which is effectively a measure of the stratification against which turbulence must work to stir the fluid. The chosen method can affect not only R_f, but the values of the nondimensional parameters that R_f depends on.

2 Methods

The DNS dataset of Arthur et al. (2016) includes results from 8 breaking wave cases with varying interface thickness (and thus varying stratification), but with similar incoming wave properties. From this data, turbulent dissipation and irreversible mixing quantities are calculated as follows. Turbulent dissipation is defined as

$$\epsilon_k^t = 2\nu\overline{s'_{ij}s'_{ij}}, \tag{1}$$

where $s'_{ij} = ((\partial u'_i/\partial x_j) + (\partial u'_j/\partial x_i))/2$ is the turbulent rate-of-strain tensor. Irreversible turbulent mixing is defined generally as

$$\epsilon_p^t = \kappa \frac{\overline{|\nabla b'|^2}}{N^2}, \tag{2}$$

where $b = g(\rho - \rho_0)/\rho_0$ is the buoyancy field and κ is the molecular diffusivity of density. In equations (1) and (2), the overbar denotes a lateral average (in the x_2 direction), while the prime denotes a departure from that average. Calculations of ϵ_k^t and ϵ_p^t are therefore functions of x_1, x_3, and t.

The buoyancy frequency N is calculated in two ways in order to explore its effect on quantifying turbulent energetics. First, following Scotti and White (2014), $N = N^*$, where N^* is the buoyancy frequency of the background density field ρ^*. The background density field represents the lowest possible potential energy state of the system if it were to be adiabatically rearranged (Winters et al., 1995), and is obtained numerically by sorting the full three-dimensional density field ρ at each time step. Changes in the background potential energy can only occur due to molecular (or numerical) diffusion, and are therefore irreversible. When irreversible mixing is calculated using $N = N^*$ in equation (2), it is denoted ϵ_p^{t*}.

The ability to calculate the background buoyancy frequency N^* using the three-dimensionally resorted density field represents an advantage of DNS that is not possible using observational data. For this reason, N is often determined by resorting a vertical density profile through a turbulent patch. As in Smyth et al. (2001) and Mater et al. (2013), virtual profiles can be taken through a DNS domain in order to mimic calculations that would be made with observational data. An alternative definition is therefore $N = \hat{N}^*$, where $\hat{N}^* = \sqrt{-(g/\rho_0)\partial\hat{\overline{\rho}}^*/\partial x_3}$ and $\hat{\overline{\rho}}^*$ represents an adiabatic rearrangement of the laterally-averaged vertical density profile at each x_1 grid point in the DNS domain at each time step. When irreversible mixing is calculated using $N = \hat{N}^*$ in equation (2), it is denoted $\hat{\epsilon}_p^t*$.

Using the definitions in equations (1) and (2), an irreversible flux Richardson number can be calculated generally as (e.g., Scotti and White, 2014)

$$R_f^* = \epsilon_p^t/(\epsilon_p^t + \epsilon_k^t). \tag{3}$$

It should be noted that this is a preferable measure of mixing efficiency to the previous definition of R_f in section 1, which can include reversible turbulent buoyancy fluxes and is therefore not fully irreversible (Venayagamoorthy and Koseff, 2016). Here, we denote the irreversible flux Richardson number calculated with ϵ_p^{t*} (using $N = N^*$ in equation 2) as R_f^*, and that calculated with $\hat{\epsilon}_p^t*$ (using $N = \hat{N}^*$ in equation 2) as $\hat{R}_f^*$.

In order to examine the effect of stratification on the irreversible mixing efficiency, and how this changes for different methods of calculating N, turbulence data are examined as a function of

$$Re_b = \epsilon_k^t/\nu N^2. \tag{4}$$

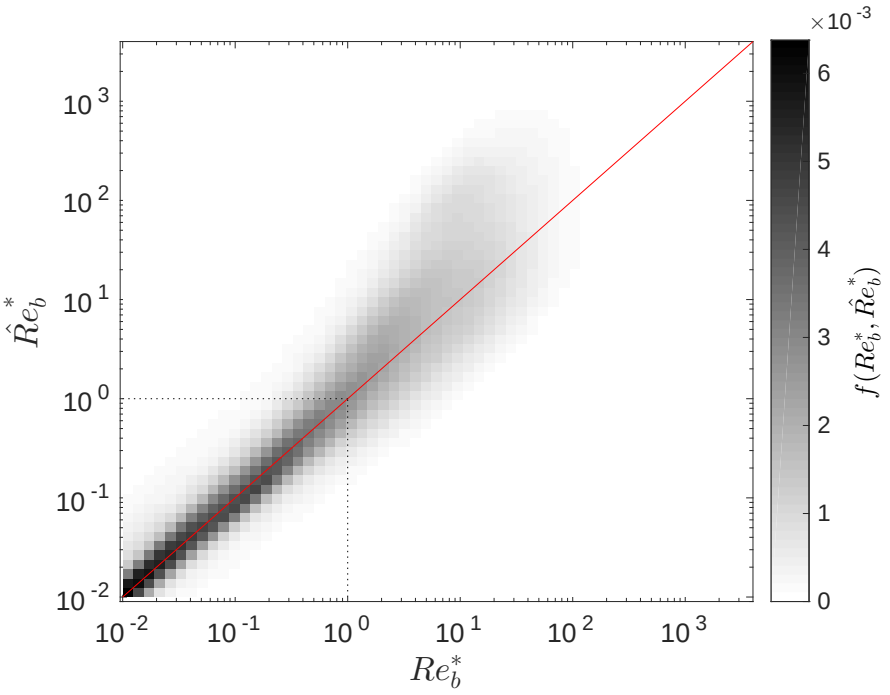

Figure 2: Comparison of Re_b^* and $\hat{Re}_b^*$ calculations.

Known as the buoyancy Reynolds number or the turbulence activity number, Re_b quantifies the scale separation between the smallest turbulent eddies that feel stratification and the Kolmogorov scale, and has been employed in the field (e.g., Davis and Monismith, 2011; Walter et al., 2014), laboratory (e.g., Barry, 2002) and in DNS (e.g., Shih et al., 2005). In what follows, Re_b values calculated with $N = N^*$ are denoted Re_b^*, while those calculated with $N = \hat{N}^*$ are denoted $\hat{Re}_b^*$.

3 Results

Turbulence quantities are considered at each (x_1,x_3,t) for all 8 breaking wave cases in Arthur et al. (2016). Due to the nonuniformity of the computational grid, each data point is weighted by the (x_1,x_3) area of the grid cell. R_f^* is thus calculated as a weighted mean, over the entire dataset, in each Re_b bin. To show the spread of the data, the area-weighted frequency of occurrence f is also calculated in each Re_b bin; f can be thought of as the probability of finding a data point within a given bin.

Since Re_b is itself a function of the buoyancy frequency N, it is first instructive to see how it varies with the calculation of N. A direct comparison may be made using a two-dimensional histogram of $f(Re_b^*, \hat{Re}_b^*)$ (figure 2), which shows that $\hat{Re}_b^*$ is generally greater than Re_b^*, especially for $Re_b > 1$. Because ϵ_k^t is not a function of N, this indicates that $\hat{N}^*$ is generally less than N^*. As a result, $\hat{R}_f^*$, which reaches a peak of nearly 0.6 for $\hat{Re}_b^* \approx 10^3$ is generally larger than R_f^*, which has maximum values between 0.2 and 0.3 for $Re_b^* < 10^2$ (figure 3a). For $Re_b^* > 10^2$, a sharp drop in the mixing efficiency occurs

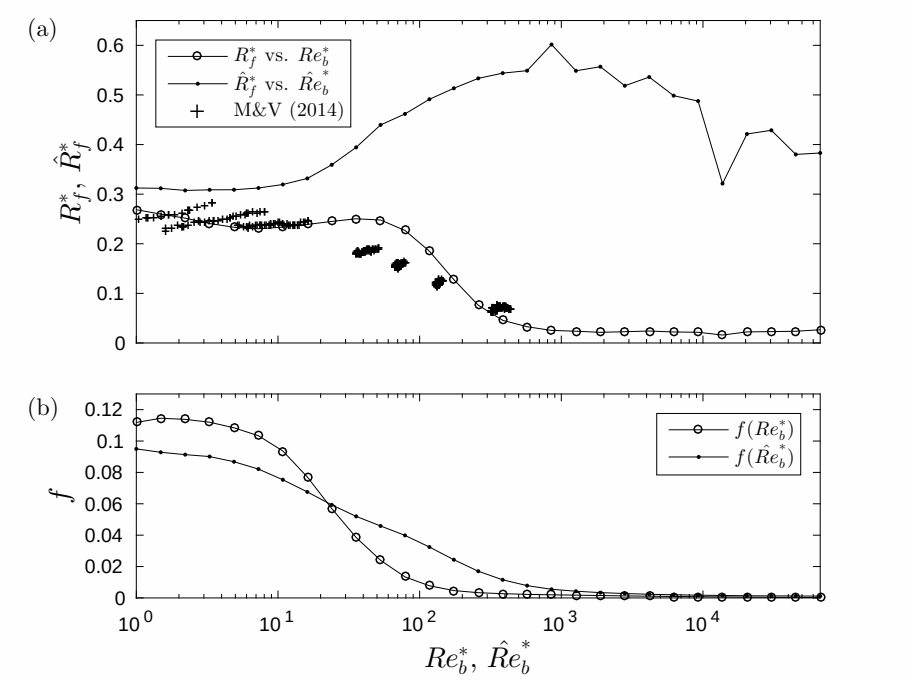

Figure 3: (a) Comparison of mean R_f^* as a function of Re_b^* to mean $\hat{R}_f^*$ as a function of $\hat{Re}_b^*$. The $\hat{R}_f^*$ calculation of Mater and Venayagamoorthy (2014) using the data of Shih et al. (2005) is included as well. (b) The area-weighted frequency of occurrence f in each Re_b^* or $\hat{Re}_b^*$ bin.

and R_f^* approaches 0. A similar result was found for R_f by Shih et al. (2005), Walter et al. (2014), and others; see figure 12 in Walter et al. (2014). Because $\hat{Re}_b^*$ is generally larger than Re_b^*, the decline of $\hat{R}_f^*$ for large values of $\hat{Re}_b^*$ occurs at a larger value of $\hat{Re}_b^*$, approximately $\hat{Re}_b^* = 10^3$. It should be noted that calculations of R_f for these large values of Re_b are based on only a small subset of the data (figure 3b), which likely explains the wiggles in the $\hat{R}_f^*$ vs. $\hat{Re}_b^*$ curve. Due to computational restrictions on Re_b associated with DNS, much of the data have relatively low (non-turbulent) values of $Re_b < 1$ (figure 2). Since these values imply laminar flow, they are omitted in figure 3.

The $\hat{R}_f^*$ calculations of Mater and Venayagamoorthy (2014) as a function of $\hat{Re}_b^*$ using the data of Shih et al. (2005) are also included in figure 3a for comparison. Their $\hat{R}_f^*$ vs. $\hat{Re}_b^*$ curve generally follows the present R_f^* vs. Re_b^* curve, but is quite different from the present $\hat{R}_f^*$ vs. $\hat{Re}_b^*$ curve. This difference may be due to the homogeneous nature of the turbulence studied by Shih et al. (2005), which could allow $\hat{N}^*$ to be a more appropriate measure of the effective stratification. In the inhomogeneous flow studied here, $\hat{N}^*$ varies spatially, and might therefore be a less appropriate measure of N. Ultimately, we find that in the present breaking wave case, using $\hat{N}^*$ leads to a relatively large mixing efficiency because the effective stratification against which the turbulence is working is relatively weak, as compared to N^*.

4 Conclusions

In this study, the irreversible mixing efficiency R_f^* of breaking internal waves on slopes was examined as a function of the buoyancy Reynolds number Re_b. Two different methods of calculating the buoyancy frequency N, one based on a three-dimensionally resorted density field and the other based on locally-resorted vertical density profiles, were used to demonstrate its importance in quantifying the mixing efficiency. In addition to changing the value of R_f^*, it was shown that different methods of calculating N produce different values of Re_b as well. This has implications for how existing parameterizations of mixing in the ocean are used: the method of calculating N not only affects the mixing efficiency, but adds some uncertainty to its estimation using Re_b-based parameterizations because this values also depends on N.

References

Arthur, R. S., Koseff, J. R., and Fringer, O. B. (2016). Local vs. volume-integrated turbulence and mixing in breaking internal waves on slopes. *J. Fluid Mech.* submitted.

Barry, M. E. (2002). *Mixing in stratified turbulence*. PhD thesis, University of Western Australia, Centre for Water Research.

Bouffard, D. and Boegman, L. (2013). A diapycnal diffusivity model for stratified environmental flows. *Dynam. Atmos. and Oceans*, 61:14–34.

Davis, K. A. and Monismith, S. G. (2011). The modification of bottom boundary layer turbulence and mixing by internal waves shoaling on a barrier reef. *J. Phys. Oceanogr.*, 41(11):2223–2241.

Ivey, G. N. and Imberger, J. (1991). On the nature of turbulence in a stratified fluid. part i: The energetics of mixing. *J. Phys. Oceanogr.*, 21(5):650–658.

Lozovatsky, I. D. and Fernando, H. J. S. (2013). Mixing efficiency in natural flows. *Philos. Trans. R. Soc. A*, 371:20120213.

Mater, B. D., Schaad, S. M., and Venayagamoorthy, S. K. (2013). Relevance of the thorpe length scale in stably stratified turbulence. *Phys. Fluids*, 25:076604.

Mater, B. D. and Venayagamoorthy, S. K. (2014). The quest for an unambiguous parameterization of mixing efficiency in stably stratified geophysical flows. *Geophys. Res. Lett.*, 41(13):4646–4653.

Munk, W. and Wunsch, C. (1998). Abyssal recipes ii: energetics of tidal and wind mixing. *Deep Sea Res.*, 45(12):1977–2010.

Osborn, T. R. (1980). Estimates of the local rate of vertical diffusion from dissipation measurements. *J. Phys. Oceanogr.*, 10(1):83–89.

Scotti, A. and White, B. (2014). Diagnosing mixing in stratified turbulent flows with a locally defined available potential energy. *J. Fluid Mech.*, 740:114–135.

Shih, L. H., Koseff, J. R., Ivey, G. N., and Ferziger, J. H. (2005). Parameterization of turbulent fluxes and scales using homogeneous sheared stably stratified turbulence simulations. *J. Fluid Mech.*, 525:193–214.

Smyth, W. D., Moum, J. N., and Caldwell, D. R. (2001). The efficiency of mixing in turbulent patches: Inferences from direct simulations and microstructure observations. *J. Phys. Oceanogr.*, 31(8):1969–1992.

Venayagamoorthy, S. K. and Koseff, J. R. (2016). On the flux richardson number in stably stratified turbulence. *J. Fluid Mech.*, 798, R1:1–10.

Walter, R. K., Squibb, M. E., Woodson, C. B., Koseff, J. R., and Monismith, S. G. (2014). Stratified turbulence in the nearshore coastal ocean: Dynamics and evolution in the presence of internal bores. *J. Geophys. Res.*, 119(12):8709–8730.

Winters, K. B., Lombard, P. N., Riley, J. J., and D'Asaro, E. A. (1995). Available potential energy and mixing in density-stratified fluids. *J. Fluid Mech.*, 289:115–128.

Wunsch, C. and Ferrari, R. (2004). Vertical mixing, energy, and the general circulation of the oceans. *Annu. Rev. Fluid Mech.*, 36:281–314.